Available online at www.sciencedirect.com
SCIENCE DIRECT®
Journal of Photochemistry and Photobiology A: Chemistry 172 (2005) 89–96
Journal of Photochemistry and Photobiology A:Chemistry
www.elsevier.com/locate/jphotochem

The effect of operational parameters on the photocatalytic degradation of three textile azo dyes in aqueous TiO_2 suspensions

Mohammad Hossein Habibi*, Ali Hassanzadeh, Shahla Mahdavi

Department of Chemistry, University of Isfahan, Hezar Jerib Street, Isfahan, 81745-73441, Iran

Received 29 June 2004; received in revised form 14 September 2004; accepted 18 November 2004
Available online 19 January 2005

Abstract

Photocatalytic degradation of three commercial textile diazo dyes, called (C.I. Direct 80, 3BL, C.I. Direct Blue 160, RL and C.I. Reactive Yellow 2, X6G) were investigated using commercial TiO_2 in aqueous solution under 400 W high-pressure mercury lamp irradiation. The effect of oxygen, temperature, catalyst loading, UV-light irradiation time, solution pH and inorganic ions such as SO_4^{2-}, Cl^- and NO_3^- were studied and optimized values were obtained. Results show that the employment of efficient photocatalyst and selection of optimal operational parameters may lead to complete decolorization and to substantial decrease of the chemical oxygen demand (COD) of dye solutions.

Keywords: UV-photodegradation; Titanium dioxide; Diazo dyes

---

1. Introduction

Azo dyes are a versatile class of colored organic compounds that have extensively been used in both industry for applications such as textiles, papers, leathers, gasoline, additives, foodstuffs and cosmetics and analytical chemistry [1,2]. About a half of global production of synthetic textile dyes (700,000 t per year) are classified into azo compounds that have the chromophore of –N=N– unit in their molecular structure and over 15% of the textile dyes are lost in wastewater stream during dyeing operation. These azo dyes are known to be largely non-biodegradable in aerobic conditions and to be reduced to more hazardous intermediates in anaerobic conditions [3]. It is well known that soluble azo dyes when incorporated into the body are split into corresponding aromatic amines by liver enzymes and intestinal flora, which can cause cancer in human. Removing color from wastes is often more important than the other colorless organic substances, because the presence of small amounts of dyes (below 1 ppm) is clearly visible and influences the water environment considerably. Therefore, it is necessary to find an effective method of wastewater treatment in order to remove color from textile effluents [4]. One of the new methods of wastewater treatment containing dyes is their photocatalytic degradation in solutions illuminated with UV-irradiation, which contains a suitable photocatalyst, mainly TiO_2. This method was successfully applied to the decomposition of numerous organic substances, including azo and anthraqinonic dyes [5]. The aim of the present work is to investigate the influence of various parameters on photocatalytic degradation of three textile diazo dyes, called (C.I. Direct 80, 3BL, C.I. Direct Blue 160, RL and C.I. Reactive Yellow 2, X6G), in the presence of TiO_2 irradiated by the UV-light. In this paper, we also examined the effects of several types of inorganic ions (e.g. SO_4^{2-}, Cl^- and NO_3^-) that are common in synthetic dye-containing effluent on the photocatalytic degradation of these diazo dyes in aqueous TiO_2 suspensions.

---

* Corresponding author. Tel.: +98 311 7932707; fax: +98 311 6689732.
E-mail addresses: habibi@chem.ui.ac.ir, habibi@sci.ui.ac.ir (M.H. Habibi).

1010-6030/$ – see front matter © 2004 Elsevier B.V. All rights reserved.
doi:10.1016/j.jphotochem.2004.11.009

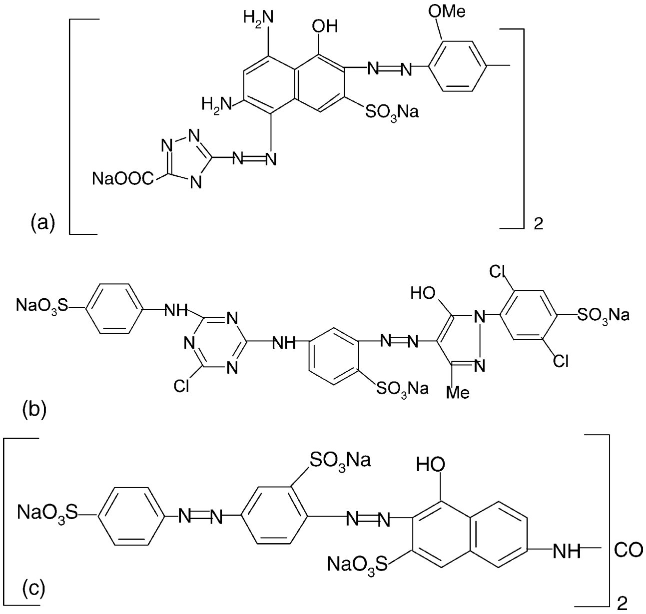

Fig. 1. (a) Chemical structure of commercial diazo dye of direct Copper Navy Blue *RL* (C.I. Direct Blue 160). (b) Chemical structure of commercial diazo dye of light Yellow *X6G* (C.I. Reactive Yellow 2). (c) Chemical structure of commercial diazo dye of Solophenyl red *3BL* (C.I. Direct 80).

2. Experimental

2.1. Reagents and materials

Solophenyl red *3BL* (C.I. Direct 80, M.W. = 1373 g/mol), Direct Copper Navy Blue *RL* (C.I. Direct Blue 160, M.W. = 1110 g/mol) and Light Yellow *X6G* (C.I. Reactive Yellow 2, M.W. = 872.5 g/mol) textile dyes were obtained from Ciba-Geigy (UK), Youhao (China) and Bitterfeld (Germany), respectively. Dyes chemical structures were shown in Fig. 1(a–c). The other materials such as K_2HPO_4, KH_2PO_4, NaOH, HCl, KCl, H_2O_2, HgI_2, KI, $Na_2B_4O_7{\cdot}10H_2O$, $KHC_8H_4O_4$, $HgSO_4$, NaCl, Na_2SO_4, $NaNO_3$, $K_2Cr_2O_7$, $C_{12}H_8N_2$, $Fe(NH_4)_2(SO4)_2{\cdot}6H_2O$, Ag_2SO_4, H_2SO_4, $FeSO_4{\cdot}7H_2O$, $AgNO_3$, $Ba(NO_3)_2$ and $C_{12}H_{11}N$ were obtained from Merck. The commercially available TiO_2 powder was anatase in crystalline form and it has a surface area about 50 m^2/g and primary particle size of 30 nm was obtained from Aldrich.

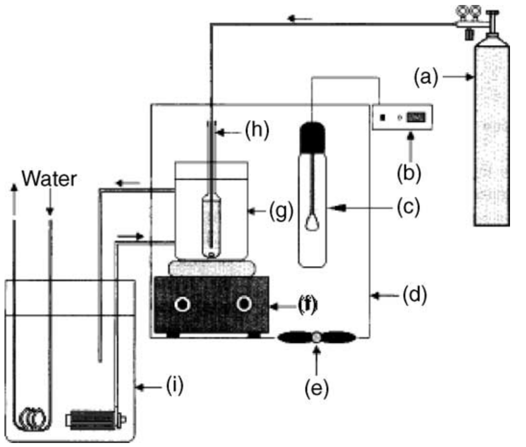

Fig. 2. Photodegradation set up for diazo dyes: (a) oxygen cylinder; (b) power supply; (c) 400 W high-pressure Hg lamp; (d) photoreactor with aluminium foil as reflector for a full irradiate of catalyst; (e) fan; (f) magnet stirrer; (g) 2 l Pyrex beaker; (h) photodegradation cell; (i) water thermostat Haake model F-122.

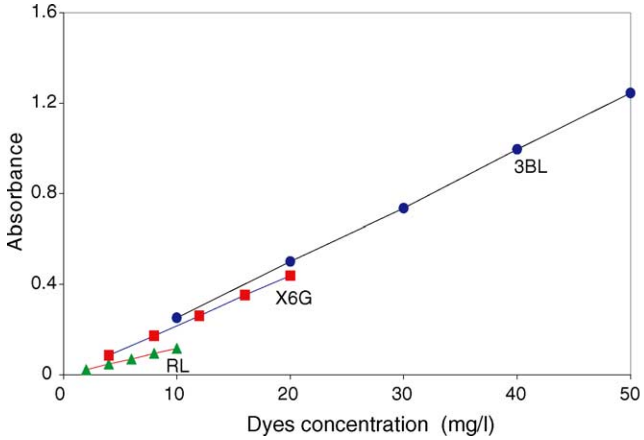

Fig. 3. Calibration curves of RL, 3BL and X6G dyes.

2.2. Apparatus

Double beam UV–visible spectrophotometer (Varian Cary 500 Scan) was used for spectrophotometric determination of diazo dyes concentrations. Photodegradation process was performed in a photodegradation cell of 200 ml in volume with a high pressure mercury lamp 400 W are shown in Fig. 2.

2.3. Experiments procedure

Fresh dye solutions were prepared before use and diluted according to the requirements of the experiments and adjusted to known pH. The photodegradation cell was feed with 100 ml of the solution with stirring. During irradiation, agitation was maintained to keep the suspension homogenous. Samples (ca. 2 ml) were withdrawn for UV–visible analysis and centrifuged for 20 min at the rate 1000 rpm. The concentration of dyes in each degraded sample were determined by a spectrophotometer at (RL; λ_{max} = 570 nm, X6G; λ_{max} = 400 nm and 3BL; λ_{max} = 530 nm), respectively, and using a calibration curve (Fig. 3). λ_{max} values applied in the absorbance measurements of dye solutions were experimentally characterized on the basis of determined UV–visible spectra (not shown in here). The measurements were also made in quartz cells at $l = 1$ cm. The linearity of the absorption curves against dye concentrations show that the absorption of these dyes obeys from the Beer's law over these dye concentrations and differences in those slopes is due to its different absorption coefficients. It is worth to note that in the cases of RL and X6G dyes that initial dye concentrations do not fall in the represented calibration curve; we have to dilute those samples which were withdrawn for concentration analysis purposes because of the Beer's law limitation in higher concentration. The control experiments were carried out as follows: (i) with dyes solutions without TiO_2 loading in the absence of UV–visible light (darkness), (ii) with dyes solutions without TiO_2 loading in the presence of visible light, (iii) with dyes solutions and TiO_2 loading in the absence of visible light, (iv) with dyes solutions and TiO_2 loading in the presence of visible light, (vi) with dyes solutions in the presence of UV-light without TiO_2 loading.

2.4. Final products

Some ionic species such as NH_4^+, NO_3^-, NO_2^-, SO_4^{2-} and Cl^- and gases such as CO_2, CO, SO_2, N_2O and NO_2 may result during dyes photocatalytic degradation. The ionic species content such as NH_4^+ is determined using Nessler regent, NO_2^- and NO_3^- after degradation are determined by using UV–visible spectrophotometer colorimetrically and SO_4^{2-} and Cl^- concentrations were determined by standard procedure [6,7].

3. Results and discussion

3.1. Effect of oxygen

In order to observe dye solution oxygen effect on the time of complete photocatalytic degradation of RL, X6G and 3BL dyes, some experiments were carried out by varying the flux of oxygen. The temperature of experiments was maintained at 25 °C by water circulation and TiO_2 photocatalyst amount was kept at 0.1 g/l. The obtained results were shown in the Fig. 4. It can be seen that the time of complete photocatalytic degradation of RL and X6G dyes in the absence of oxygen are relatively high (120 and 90 min, respectively) but by increasing oxygen flux the complete photocatalytic degradation time of these dyes were decreased. In other words, the oxygen is necessary for photocatalytic degradation of RL and X6G dyes. In contrast, the influence of oxygen flux variation on the time of complete photocatalytic degradation of 3BL dye was not significant and photocatalytic degradation of this dye well progressed in the absence of oxygen. It seemed that the oxygen was probably not necessary for 3BL dye photocatalytic degradation. It is worth to note that the complete photocatalytic degradation time in the whole experiments has been taken where the complete decolorization occurred and the absorbance of withdrawn dye samples were too significant to detectable by UV–visible instrument. In order to explain discrepancy between these different behaviors of dyes photocatalytic degradation, we used the following mechanisms, which have been reported in literature for photocatalytic degradation processes [8–12].

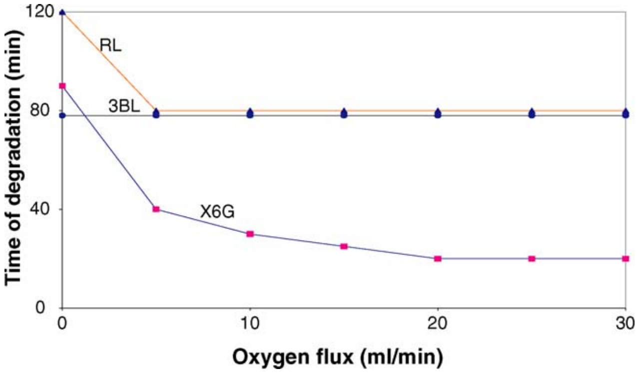

Fig. 4. Effect of oxygen flux on the complete degradation time of diazo dyes of RL, 3BL and X6G.

Mechanism (a):

$$\text{dye} + h\upsilon \rightarrow {}^1\text{dye}^* + {}^3\text{dye}^* \quad (1a)$$

$${}^1\text{dye}^* \text{ or } {}^3\text{dye}^* + TiO_2 \rightarrow \text{dye}^{\bullet+} + TiO_2(e^-) \quad (2a)$$

$$TiO_2(e^-) + O_2 \rightarrow O_2^- + TiO_2 \quad (3a)$$

$$\text{dye}^{\bullet+} \rightarrow \text{products} \quad (4a)$$

$$\text{dye}^{\bullet+} + O_2 \rightarrow \text{products} \quad (5a)$$

Mechanism (b):

$$TiO_2 + h\upsilon \rightarrow e^- + h^+ \quad (1b)$$

$$e^- + O_2 \rightarrow O_2^- \quad (2b)$$

$$H_2O + h^+ \rightarrow {}^\bullet OH + H^+ \quad (3b)$$

$$O_2 + 2H^+ + e^- \rightarrow H_2O_2 \quad (4b)$$

$$H_2O_2 + O_2^- \rightarrow {}^\bullet OH + OH^- + O_2 \quad (5b)$$

$$H_2O_2 + e^- \rightarrow {}^\bullet OH + OH^- \quad (6b)$$

$$OH^- + h^+ \rightarrow {}^\bullet OH \quad (7b)$$

Since, the whole diazo dyes have no significant degradation in the absence of TiO_2 photocatalyst even in the presence of UV-light; the mechanism (a) will be cancelled. In consequence, the mechanism (b) from the physical point of view is more feasible. The discrepancy between the effect of oxygen on the complete photocatalytic degradation time of RL and X6G dyes is due to light-limited condition. But, for the fact that oxygen did not influence the degradation of 3BL can be explained by the fact that some of the adsorbed aromatic compounds can undergo direct oxidation by electron transfer to the surface holes by following equation.

$$R_{ads} + TiO_2(h^+) \rightarrow TiO_2 + R^{\bullet+} \quad (1c)$$

and the radical cation produced in this manner can undergo hydrolysis or mesolytic bond scission to low weight products [13–15].

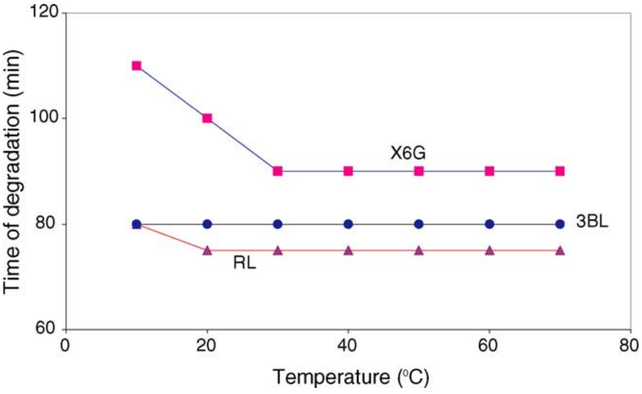

Fig. 5. Effect of solution temperature on the complete degradation time of diazo dyes of RL, 3BL and X6G.

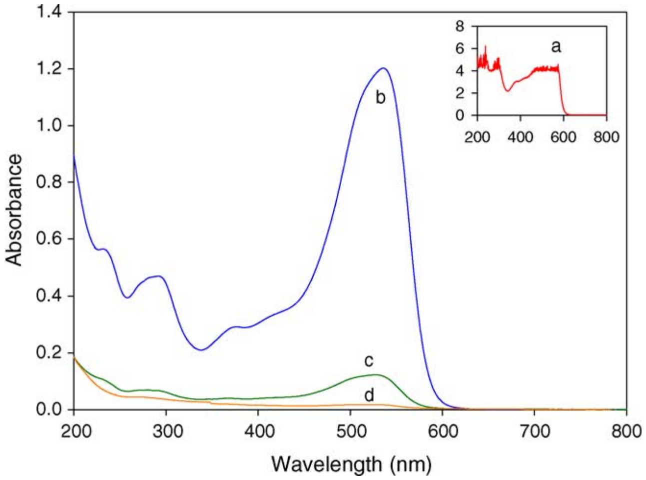

Fig. 6. UV–visible absorption spectra of Solophenyl red 3BL in water at different dye concentrations. (a) 4×10^{-3} mol dm^{-3}, (b) 4×10^{-4} mol dm^{-3}, (c) 4×10^{-5} mol dm^{-3} and (d) 4×10^{-6} mol dm^{-3}.

3.2. Effect of temperature

Fig. 5 shows the effect of solution temperature on the complete photocatalytic degradation time of three dyes at optimized oxygen flux. As shown in Fig. 5, the effect of temperature for RL and 3BL is not significant. Therefore, room temperature is selected as optimum temperature for the next experiments. In contrast, for X6G dyes molecules temperature variation is an important factor for its photocatalytic degradation. It is well known that the solution temperature can affect both photocatalyst and bulk properties including dye molecules. In addition, temperature can also affect adsorption/desorptions processes of dyes molecules on the TiO_2 photocatalyst surface. Since the band gap energy of TiO_2 is so high (ca. 3 eV); therefore, thermal excitations do not have an important role. Hence, bulk and surface phenomena can be strongly influenced with temperature variation. Some of the most important bulk phenomena are dye molecule aggregations, azo-hydrazone tautomerization and geometric (*cis–trans*) isomerization which in turn have significant roles in photocatalytic degradation and can easily be varied with temperature variation. Among these phenomena, dye molecules aggregation has the most important effect on the photocatalytic degradation yield and solution temperature elevation can cause disaggregation of dye molecules. It should be mentioned that, we did not observe any aggregation for three diazo dyes within concentration range of 10^{-3} to 10^{-6} mol dm^{-3} (Fig. 6). Therefore, in the absence of dye molecule aggregation, adsorption/desorptions processes must have the most important role in photocatalytic degradation processes. With considering molecular weight of three azo dyes, X6G (M.W. = 872.5 g/mol) is a light dye molecule in comparison with RL (M.W. = 1110 g/mol) and 3BL (M.W. = 1373 g/mol) and by taking into account the fact that X6G has three anion site (sulfate groups) in its molecular structure, while the 3BL and RL have six and four anion site (sulfate and carboxylate groups) in their molecular structure, respectively, which can interact with water molecules by ion–dipole interactions. Consequently, it seemed that the hyradation of X6G molecule is lower than those of RL and 3BL molecules. Therefore, solution temperature has significant effect on the effective collisions between X6G and TiO_2 photocatalyst as compared to3BL and RL.

3.3. Effect of TiO_2 amount

The effect of TiO_2 amount on the photocatalytic degradation of three diazo dyes was studied at optimized oxygen flux and solution temperature and obtained results were shown in Fig. 7. The photocatalytic degradation efficiency of the whole dyes was increased by increasing the photocatalyst amount, and then reaches the highest value and finally remains at constant value (i.e. became independent of the catalyst concentration). This can be rationalized in terms of availability of active sites on TiO_2 surface and the light penetration of photoactivating light into the suspension. The availability of active sites increases with the suspension of catalyst loading, but the light penetration and, hence, the photoactivated volume of the suspension shrinks [16]. Moreover, the decrease in the percentage of degradation at higher catalyst loading

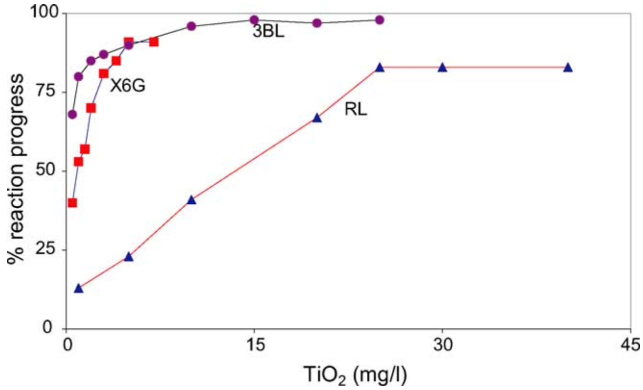

Fig. 7. Effect of TiO_2 amount on the complete degradation of diazo dyes of RL, 3BL and X6G.

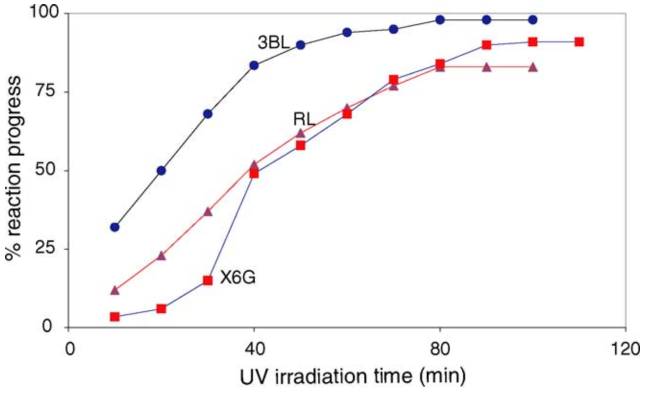

Fig. 8. Effect of UV-irradiation time on the degradation of diazo dyes of RL, 3BL and X6G.

may be due to deactivation of activated molecules by collision with ground state molecules. Shielding by TiO_2 may also take place (Eq. (1d)).

$$TiO_2{}^{*} + TiO_2 \rightarrow TiO_2{}^{\#} + TiO_2 \quad (1d)$$

where $TiO_2{}^{*}$ is the TiO_2 with active species adsorbed on its surface and $TiO_2{}^{\#}$ is the deactivated form of TiO_2 [17]. Agglomeration and sedimentation of the TiO_2 particles have also been reported. In this condition, parts of the catalyst surface become unavailable for photon absorption and dye adsorption, thus bringing little stimulation to the catalytic reaction. The crucial concentration depends on the geometry, the working conditions of the photoreactor and the type of UV-lamp (power, wavelength). The optimum amount of TiO_2 has to be added in order to avoid unnecessary excess catalyst and also to ensure total absorption of light photons for efficient photomineralization. This optimum loading of photocatalyst is found to be dependent on the initial solute concentration (ref. [16] and references therein). We have found that the most effective degradation of X6G, 3BL and RL dyes was observed with 7, 10 and 25 mg/l of TiO_2, respectively. As shown in Fig. 7, the initial slopes of linear portion of individual curves are different and this slope increment for three diazo dyes is as follows. The slope of X6G dye is greater than the 3BL dye, which in turn is greater than the RL dye, which may be due to their physicochemical properties.

3.4. *Effect of UV-irradiation time*

Fig. 8 shows the effect of UV-light irradiation time on the photocatalytic degradation of three textile diazo dyes of RL, 3BL and X6G at optimized oxygen flux, solution temperature and catalyst amount. In the presence of TiO_2 and UV-light, the 58, 62 and 90% of X6G, RL and 3BL diazo dyes were degraded at irradiation time of 50 min and it is also evident that the percentage of decolorization and photodegradation increases with increasing irradiation time. The slow kinetics of dyes degradation after certain time limit is due to: (a) the difficulty in converting the N atoms of dye into oxidized nitrogen compounds, (b) the slow reaction of short chain aliphatics with $^{\bullet}OH$ radicals and (c) the short life-time of photocatalyst because of active sites deactivation by strong by-products deposition (carbon, etc.) (ref. [16] and references therein). Discrepancy between the percent of photocatalytic degradation of three diazo dyes may be due to ability of their direct hole capturing and/or photocatalytic degradation mechanisms [13–15].

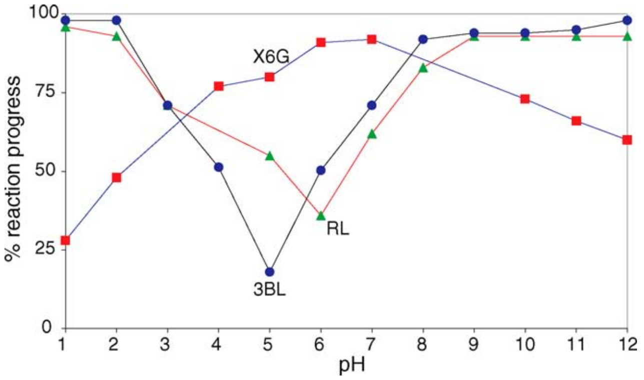

Fig. 9. Effect of solution pH on the degradation of diazo dyes of RL, 3BL and X6G.

3.5. *Effect of pH*

The effect of solution pH was studied in the range of 1–12 at optimized oxygen flux, solution temperature, catalyst amount and UV-irradiation time. Fig. 9 demonstrates the photocatalytic degradation of three diazo dyes RL, 3BL and X6G at different pH. The best results for X6G photocatalytic degradation was obtained in neutral solution (i.e. pH range from 4 to 7); whereas, for RL and 3BL dyes, the worst results were obtained in this pH range and acidic and alkaline pH were favored. The interpretation of pH effects on the efficiency of dye photocatalytic degradation process is a very difficult task because of its multiple roles. First, is related to the ionization state of the surface according to the following reactions,

$$TiOH + H^{+} \Leftrightarrow TiOH_2{}^{+} \quad (1e)$$

$$TiOH + OH^{-} \Leftrightarrow TiO^{-} + H_2O \quad (2e)$$

as well as to that of reactant dyes and products such as acids and amines. pH changes can thus influence the adsorption of dye molecules onto the TiO_2 surfaces, an important step for the photocatalytic oxidation to take place. The point of zero charge (pzc) of the TiO_2 (Degussa P25) is at $pH = 6.8$. Thus, the TiO_2 surface is positively charged in acidic media ($pH < 6.8$); whereas, it is negatively charged under alkaline conditions ($pH > 6.8$). Second, hydroxyl radicals can be formed by the reaction between hydroxide ions and positive holes. The positive holes are considered as the major oxidation species at low pH; whereas, hydroxyl radicals are considered as the predominant species at neutral or high pH levels. It was stated that in alkaline solution $^{\bullet}OH$ are easier to be generated by oxidizing more hydroxide ions available on TiO_2 surface; thus, the efficiency of the process is logically enhanced. Although it should be noted that in alkaline solution there is a Coulombic repulsion between the negative charged surface of photocatalyst and the hydroxide anions. This fact could prevent the formation of $^\bullet$OH and thus decrease the photooxidation but very high pH has been found favorable even when anionic azo dyes should hamper adsorption on the negatively charged surface. At low pH, reduction by electrons in conduction band may play a very important role in the degradation of dyes due to the reductive cleavage of azo bonds. Third, the TiO_2 particles tend to agglomerate under acidic condition and the surface area available for dye adsorption and photon absorption would be reduced. Hence, pH plays an important role both in the characteristics of textile waters and in the reaction mechanisms that can contribute to dye degradation, namely hydroxyl radical attack, direct oxidation by the positive hole and direct reduction by the electron in the conducting band. An additional explanation for the pH effects can be related with changes in the specification of the dye. That is, protonation or deprotonation of the dye can change its adsorption characteristics and redox activity [16]. Discrepancies between photocatalytic degradation behavior of three diazo dyes can be explained by the facts that, for X6G molecules adsorbed at lower pH completely which is due to strong Coulombic attraction onto photocatalyst which did not take place in the cases of RL and 3BL. Therefore, for X6G in the lower pH instead of photocatalytic degradation process only fully adsorption take place which in turn blocked all active TiO_2 sites and impeded further photocatalytic degradation. Since the whole dyes were anionic; therefore, due to Coulombic repulsion in higher solution pH, the X6G dye was scarcely adsorbed. Therefore, the photocatalytic degradation of this dye was decreased by increasing solution pH. But for the above mentioned reasons the photocatalytic activity of anionic dyes (mainly sulfonated dyes) such as RL and 3BL reached a maximum value in alkaline conditions (pH range 8–12). Furthermore, by decreasing the pH of dye solution to less than 0.01 the 3BL dye molecules tend to form J-aggregate (Fig. 10). In contrast, RL and X6G dye molecules were coagulated in this lower pH instead of aggregation.

3.6. *Effect of inorganic ions*

Fig. 11 demonstrates the effect of $SO_4{}^{2-}$ ions concentration on the photocatalytic degradation of three diazo dyes of RL, 3BL and X6G in the presence of TiO_2 under UV-light irradiation at optimized oxygen flux, solution temperature, catalyst amount, UV-irradiation time and pH conditions. By increasing the $SO_4{}^{2-}$ concentration, the photocatalytic degradation of three diazo dyes of RL, 3BL and X6G was decreased. Similar trends were observed for Cl^- and $NO_3{}^-$ ions (not shown here). These anions inhibited the activity of the photocatalyst (TiO_2) by trapping h^+ and $^\bullet$OH under both acidic and basic conditions [18]. It is worth to note that the occurrence of dissolved inorganic ions is rather common in dye containing industrial wastewaters. Anions, such as $SO_4{}^{2-}$, Cl^- and $NO_3{}^-$ could be adsorbed on the TiO_2 surface in acidic conditions by electrostatic attraction. In alkaline solutions, such adsorption would be unlikely because of repulsive electrostatic force [18].

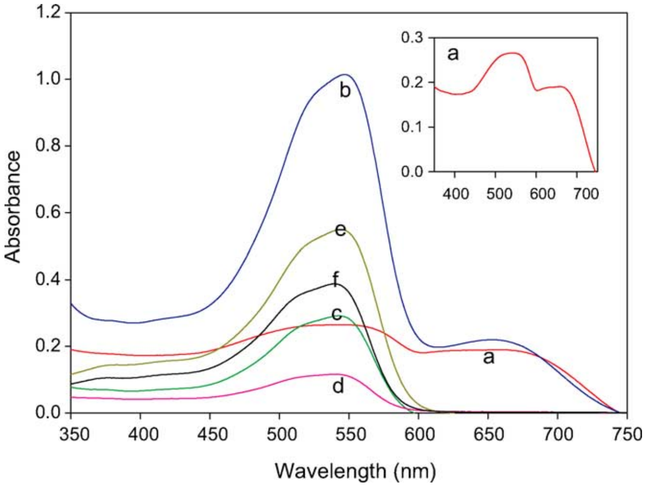

Fig. 10. Absorption spectra of aggregated Solophenyl red 3BL aqueous solution (4×10^{-5} mol dm^{-3}) at different pH after 10 h: (a) less than 1.14, (b) 1.14, (c) 3.00, (d) 4.20, (e) 7.32 and (f) 11.90.

3.7. *Kinetics study of photocatalytic degradation*

The photocatalytic degradation of some many organic compounds in TiO_2 suspensions under UV-light illumination has often been modeled to the Langmuir–Hinshelwood rate law (Eq. (1f)), which also covers the adsorption properties of the substrate on the photocatalyst surface [14].

$$\text{rate} = \frac{-\mathrm{d}C}{\mathrm{d}t} = \frac{k_{\mathrm{L-H}} K_{\mathrm{ads}} C}{1 + K_{\mathrm{ads}} C} \tag{1f}$$

where $k_{\mathrm{L-H}}$ is the reaction rate constant in mol dm^{-3} min^{-1}; K_{ads} the adsorption coefficient of the reactant on TiO_2 in (mol dm^{-3})$^{-1}$; and C is the concentration of the solute in mol dm^{-3}. The values of $k_{\mathrm{L-H}}$ and K_{ads} are used to explain the coefficients defining the rate determining reaction events and pre-equilibrium adsorption within an adsorbed monolayer at

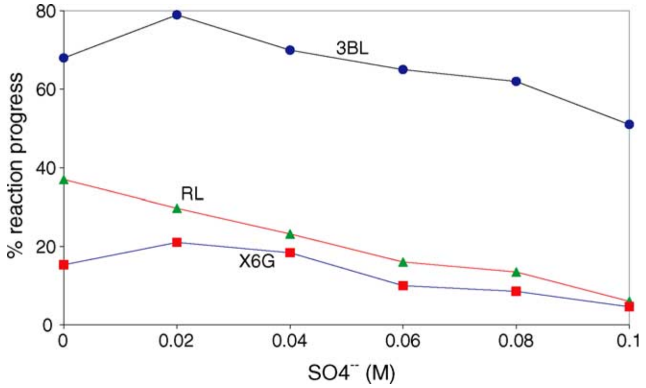

Fig. 11. Effect of inorganic ions on the degradation of diazo dyes of RL, 3BL and X6G.

Table 1
Pseudo-first-order kinetic parameters of three diazo dyes photocatalytic degradation

Dye	R^2	k (min^{-1})	$t_{1/2}$ (min)
RL	0.9986	0.0272	25.4779
X6G	0.9776	0.0305	22.7213
3BL	0.9976	0.0261	26.5517

the oxide surface and the aqueous solution interface. The effect of light intensity is also incorporated in $k_{\text{L–H}}$ and K_{ads} especially expresses the equilibrium constant for fast adsorption–desorption processes between surface monolayer and bulk solution [14]. Integration of Eq. (1f) yields the following equation:

$$\ln\left(\frac{C_0}{C}\right) + K(C_0 - C) = k_{\text{L–H}} K_{\text{ads}} t \qquad (2f)$$

When the initial concentration C_0 is small, Eq. (2f) changes to Eq. (3f), which expresses a pseudo-first-order reaction kinetic regime.

$$\ln\left(\frac{C_0}{C}\right) = k_{\text{L–H}} K_{\text{ads}} t = kt \qquad (3f)$$

yielding half-life, $t_{1/2}$ (in min) is

$$t_{1/2} = \frac{0.693}{k} \qquad (4f)$$

where k is the pseudo-first-order reaction rate constant, $k = k_{\text{L–H}} \times K_{\text{ads}}$ in min^{-1}. The photocatalytic degradation of RL, 3BL and X6G dyes as a function of the irradiation time was observed to follow an exponential decay like form as depicted in Fig. 12a. Besides, a plot of $\ln(C_0/C)$ versus time for the whole dyes in the optimized conditions was also linear (Fig. 12b), suggesting that the photodegradation reaction follows the pseudo-first-order reaction kinetics. The pseudo-first-order reaction rate constant and half-life parameters for three diazo dyes were listed in Table 1. Discrepancy between the pseudo-first-order reaction rate constants may be due to different photocatalytic degradation mechanisms and/or is owing to a competition for degradation between the reactant and the intermediate products.

3.8. Mineralization studies of diazo dyes

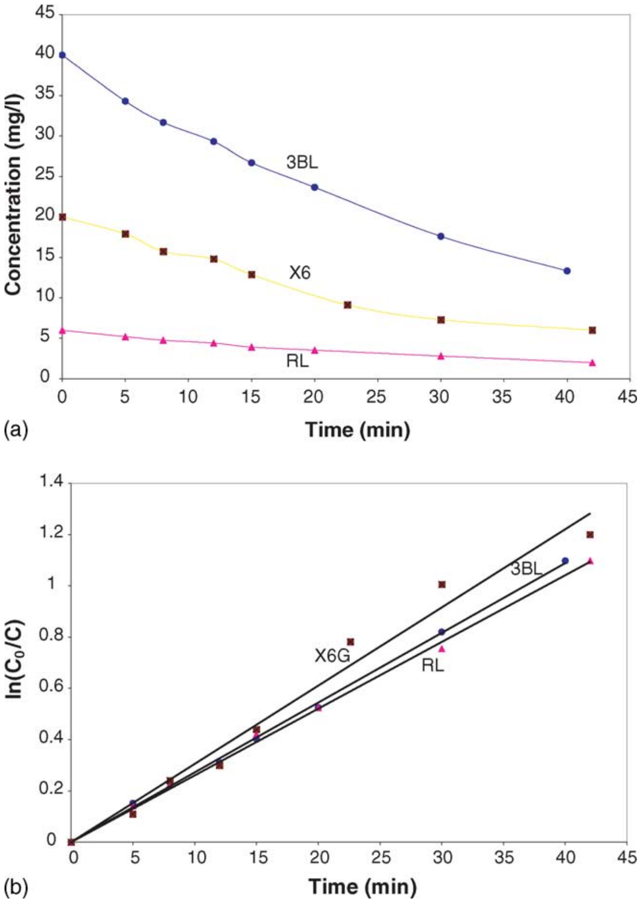

Fig. 12. (a) The photocatalytic degradation of RL, 3BL and X6G as a function of the irradiation time. (b) Kinetic study of photocatalytic degradation of three diazo dyes of RL, 3BL and X6G.

The oxidative mineralization process was followed by chemical oxygen demand (COD) disappearance (Fig. 13). COD was measured as a function of UV-irradiation time using standard acidic dichromate method [7]. The COD curve of X6G has a sigma shape indicating that it is related to the formation of final products. The inflection point corresponds to a reaction time of ca. 40 min, which is equal to the major part of X6G disappearance. It could correspond to the aromatic rings opening with the transient formation of carboxylic acids followed by the evolution of CO_2 according to the “photo-Kolbe” reaction [14].

$$\text{R–COO}^- + \text{h}^+ \rightarrow \text{R} + CO_2 \qquad (1g)$$

The results presented in Fig. 13 also showed that the photocatalytic process leads, apart from decolorization, to a substantial decrease of the COD of solution for the whole

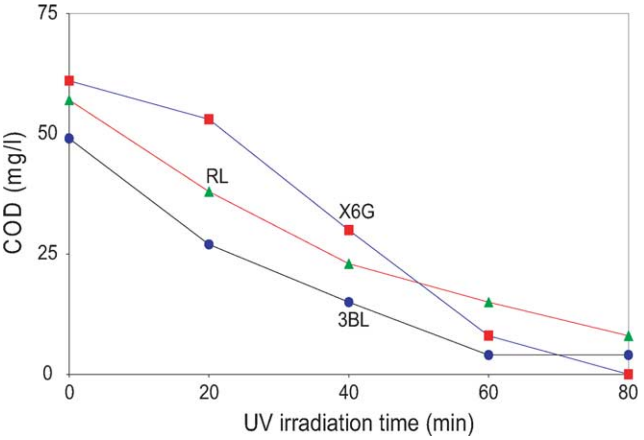

Fig. 13. COD values against UV-irradiation time of three diazo textile dyes of RL, 3BL and X6G.

azo dyes. It is observed however that this decrease is much slower for 3BL and RL dyes than the degradation of X6G since the COD curve lags the dye concentration curve considerably. This is due to the formation of smaller uncolored products [19], during the degradation of 3BL and RL dyes, which continue to contribute to the COD of the solution. To achieve complete degradation of the smaller organic compounds, longer irradiation time is required; therefore, it seemed that the complete mineralization occur for X6G dye while for 3BL and RL dyes partial mineralization is take place.

4. Conclusion

The progress of photocatalytic degradation of three diazo dyes RL, 3BL and X6G was monitored by the changes in substrate concentration of dyes by measuring the absorbance with UV–visible spectrophotometer. Results indicate that the photocatalytic degradation of three dyes in water on TiO_2 photocatalyst are very different and depend on the concentration of dye, oxygen flux, solution temperature, amount of photocatalyst, UV-irradiation time, solution pH and inorganic ions concentration. The difference was due to the difference in physicochemical properties of three diazo dyes. In addition, the presence of inorganic ions such as SO_4^{2-}, Cl^- and NO_3^- that are frequently found to co-exist with azo dyes in industrial effluent generally decreased the photocatalytic degradation rate of the whole dyes. The complete mineralization was confirmed using the chemical oxygen demand measurements and formation of inorganic ions such as NH_4^+, NO_3^-, NO_2^-, Cl^- and SO_4^{2-}.

Acknowledgements

This work was supported Isfahan University, Graduate School. The authors are grateful for their support.

References

[1] M. Dakiky, I. Nemcova, Dyes Pigments 44 (2000) 181–193.
[2] M. Bhaskar, A. Gnanamani, R.J. Ganeshjeevan, R. Chandraskar, S. Sadulla, G. Radhakrishnan, J. Chromatogr. A 1018 (2003) 117–123.
[3] H. Park, W. Choi, J. Photochem. Photobiol. A: Chem. 159 (2003) 241–247.
[4] N. Daneshvar, D. Salari, A.R. Khataee, J. Photochem. Photobiol. A: Chem. 157 (2003) 111–116.
[5] W. Baran, A. Makowski, W. Wardas, Chemospere 53 (2003) 87–95.
[6] L. Meits, Handbook of Analytical Chemistry, 1963, p. 11-2.
[7] A.E. Greenbery, L.S. Clesceri, D. Eaton, Standard methods: For the Examination of Water and Wastewater, 18th ed., 1992, p. 550.
[8] H. Meier, J. Photochem. Photobiol. A: Chem. 16 (1972) 219.
[9] H. Gerischer, J. Photochem. Photobiol. A: Chem. 16 (1972) 243.
[10] A. Hagfeldt, M. Gratzel, Chem. Rev. 95 (1995) 49.
[11] B.A. Parkinson, M.T. Spitler, Electrochim. Acta 37 (1992) 943.
[12] S.N. Frank, A.J. Bard, J. Phys. Chem. 81 (1977) 1484.
[13] C. Gomes-da-Silva, J. Luís Faria, J. Photochem. Photobiol. A: Chem. 155 (2003) 133–143.
[14] A. Houas, H. Lachheb, M. Ksibi, E. Elaloui, C. Guillard, J. Herrmann, Appl. Catal. B: Environ. 31 (2001) 145–157.
[15] G. Sivalingam, K. Nagaveni, M.S. Hegde, G. Madras, Appl. Catal. B: Environ. 45 (2003) 23–38.
[16] I.K. Konstantinou, T.A. Albanis, Appl. Catal. B: Environ. 49 (2004) 1–14.
[17] B. Neppolian, H.C. Choi, S. Sakthivel, B. Arabindoo, V. Murugesan, J. Hazard. Mater. B89 (2002) 303–317.
[18] C. Hu, J.C. Yu, Z. Hao, P.K. Wong, Appl. Catal. B: Environ. 46 (2003) 35–47.
[19] F. Kiriakidou, D.I. Kondarides, X.E. Verykios, Catal. Today 54 (1999) 119–130.